photonics

MDPI

Article

Nonlinear Absorption and Ultrafast Dynamics of Ag Nanoparticle

Jijuan Jiang [1,2], Jun Wang [1,3], Tong Wu [1] and Yachen Gao [1,*]

[1] College of Electronic Engineering, Heilongjiang University, Harbin 150080, China; jijuanjiang@126.com (J.J.); wangjun1003@163.com (J.W.); 124wutong@163.com (T.W.)
[2] College of Communication and Electronic Engineering, Qiqihar University, Qiqihar 161000, China
[3] College of Light Industry, Harbin University of Commerce, Harbin 150028, China
* Correspondence: gaoyachen@hlju.edu.cn

Abstract: Resonant nonlinear optical absorption of silver nanoparticles was studied experimentally via open aperture Z-scan using 130 fs, 400 nm laser pulses. Experimental results show that, at low laser intensity, silver nanoparticles can exhibit saturated absorption. While at high laser intensity, it shows reverse saturated absorption. The saturable absorption is explained in terms of ground state plasmon bleaching, while the reverse saturable absorption is believed to be from two-photon absorption. Saturable optical intensity and two-photon absorption coefficient were obtained to be 1.3×10^{10} W/m^2 and 3.3×10^{-10} m/W, respectively. The energy relaxation process of Ag nanoparticles after laser excitation was studied via pump-probe technique at 400 nm. Experimental results demonstrated that energy relaxation included electron-phonon coupling process with time constant $\tau_1 = (713 \pm 50)$ fs, and phonon-phonon coupling process with time constant $\tau_2 = (25.2 \pm 3)$ ps, respectively.

Keywords: nonlinear absorption; nanoparticle; surface plasmon resonances; Z-scan; pump-probe; energy relaxation

check for updates

Citation: Jiang, J.; Wang, J.; Wu, T.; Gao, Y. Nonlinear Absorption and Ultrafast Dynamics of Ag Nanoparticle. *Photonics* **2021**, *8*, 233. https://doi.org/10.3390/photonics8070233

Received: 11 May 2021
Accepted: 19 June 2021
Published: 23 June 2021

Publisher's Note: MDPI stays neutral with regard to jurisdictional claims in published maps and institutional affiliations.

Copyright: © 2021 by the authors. Licensee MDPI, Basel, Switzerland. This article is an open access article distributed under the terms and conditions of the Creative Commons Attribution (CC BY) license (https://creativecommons.org/licenses/by/4.0/).

1. Introduction

Around specific wavelengths, noble metal nanoparticles can exhibit strong nonlinear optical properties and ultrafast response, which results in their having possible applications for photonic devices and attracting special interest [1–16]. Specially, Au and Ag nanoparticles have been the subject of most studies since both show strong surface plasmon resonance (SPR) absorption [1–16]. Moreover, SPR can induce an enhanced local field which can bring a variety of significant optical characteristics. Specially, non-linear absorption is critical because it is able to change strong light propagation in the medium, and induce many novel applications.

In Au nanoparticles, plasmon resonance absorption and interband absorption overlap partly, which substantially decreases the plasma excitation efficiency. However, for Ag, the wavelength of interband absorption is about 320 nm and the SPR wavelength is about 400 nm, leading plasmon excitation of silver nanoparticles stronger than that of Au nanoparticles. Therefore, multiple studies focused on non-linear absorption and optical limiting of Ag nanoparticles [15]. Previous study demonstrated the optical nonlinearity of silver nanodots under 532 nm picosecond pulsed laser [8]. Zheng et al. evaluated nanosecond nonlinear absorption of Ag nanowires/silica gel glass composite at 532 nm [9,10]. The nonlinear absorption of silver nano sol was investigated at 456, 477, and 532 nm by open aperture Z-scan technique [11]. These data demonstrated that saturable absorption (SA) flipped to reverse saturated absorption (RSA) behavior under higher input excitation. A parallel switching behavior was observed in ZrO_2 [12] and silver nanoparticles in polymethyl methacrylate (PMMA) [13] under 532 nm nanosecond laser pulse. This observed behavior was discussed based on different mechanisms in the literatures. Regarding to

silver nanowires/silica gel glass composite [9], the switching behavior could be explained from various environmental and electronic dynamics in both liquid and solid matrices. For silver nano sol [10], the data was interpreted by SPR bleach, photochemical alters and potential particle size selective excitation effects. While for Ag nanoparticles in ZrO_2 [12], the mechanism of this switch was proposed from the viewpoint of electron Kerr nonlinearity and non-linear light scattering.

Almost all studies above were not carried under the resonant wavelength of 400 nm. Only R.A. Ganeev et al. [14] evaluated the nonlinear optical absorption in Ag nanoparticles at 397.5 nm. Their data demonstrated that silver nanoparticles present either SA for 1.2 ps pulsed laser or RSA for 8 ns pulsed laser. As we know, non-linear optical characteristics of metal nanoparticles rely on both laser wavelength and laser pulse-width. Until now, at resonant wavelength, the optical nonlinearities of Ag nanoparticle have not been investigated in the femtosecond time scale.

Although we have previously investigated the non-linear absorption of Ag nanoparticles using 130 fs pulsed laser at 400 nm, we focused mainly on a cumulative effect on asymmetrical open-aperture Z-scan signal [15]. In fact, to further evaluate the exact processes occurring in Ag nanoparticle on laser irradiation, a time-resolved study is necessary [11]. In the current study, we study resonant non-linear absorption and dynamics process of silver nanoparticles, respectively.

2. Experiments

A Coherent Mira 900 laser system and a Coherent Legend-F regenerative amplifier were used to prepare silver nanoparticles and used as the excitation source for Z-scan measurement and pump-probe spectroscopy. The combined system provides linearly polarized, 800 nm pulsed laser with a duration of 130 fs.

The femtosecond laser was used to ablate silver metal plates to prepare silver nanoparticles [16]. In order to remove the oxide layer and prevent simultaneous oxidation, the pure silver target material is ultrasonically treated and then washed with ethanol. Silver nanoparticles are synthesized by laser ablation of a silver target placed on the bottom of a glass container which is containing 5 mL of ethanol containing 1 mg poly (N-vinyl-2-pyrrolidone) (PVP). Thirty minutes later, Ag nanoparticles dispersed in ethanol were successfully prepared. The UV-vis linear absorption spectrum of the sample was measured by USB4000 spectrometer. The shape and size of the nanoparticles was observed with a transmission electron microscope (TEM).

Non-linear absorption characteristics were researched by open-aperture Z-scan experiment [17]. The experiment performed with a 400 nm femtosecond laser obtained by doubling frequency of 800 nm laser. A lens with focal length of 15 cm is applied to focus femtosecond laser pulse to obtain $\omega_0 = 30$ μm focal spot, and the Rayleigh length is $z_0 = \pi\omega_0^2/\lambda = 7.1$ mm. The sample is filled with a quartz cuvette with 2 mm path length, $z_0 \gg L$, it accords with the approximate condition of thin medium. In order to study the nonlinear absorption properties of Ag nanoparticles, experiments were performed under different energies. The energy change is achieved through the attenuator. To avoid the cumulative effect and thermal effect, the laser repetition rate was choose to be 1 Hz [5]. Considering that the non-linearity of the quartz cuvette and the solvent may affect the experimental results, before testing the sample, we performed a Z-scan test on a quartz cuvette filled with ethanol solvent. The results show that, under the energy used in our experiment, no nonlinearity was observed.

Resonant dynamics process of Ag nanoparticles was studied using pump-probe experiment. Details of the experiment can be found in reference [18]. By frequency doubling 800 nm laser, 400 nm pulsed femtosecond laser was generated to act as pump pulse and probe pulse. A Glan–Taylor polarizer and a half wave plate were used to adjust the pulse energy. Two lenses with focal length of 40 cm and 20 cm were applied to focused pump and the probe beam, which makes the pump and the probe beam radius be 32 μm and 16 μm, respectively. A prism was mounted on a moving stage to produce the time

delay t of pump beam and the probe beam. The probe signal was sent to a digital lock-in amplifier and recorded. The differential transmission $\Delta T(t)/T$ is obtained as a function of t.

3. Result and Discussion

Figure 1 illustrated TEM image and absorption spectrum. From the TEM image of the Ag nanoparticles, the average radius was detected to be about 25 nm. From the spectrum of absorption, a strong SPR peak at 403 nm can be found. In addition, the results show that there is an increase in linear absorption in the range of 350 nm to 300 nm, which is generally considered to be caused by interband absorption [19–21].

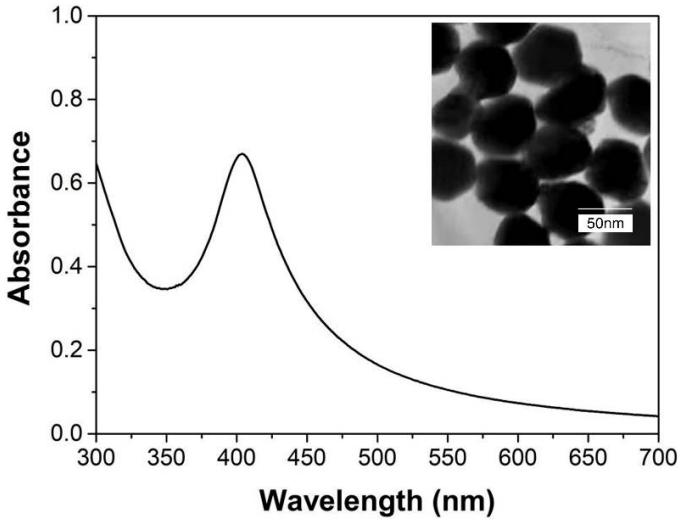

Figure 1. Spectrum of absorption spectrum and image of TEM of Ag nanoparticles.

Figures 2 and 3 displayed open aperture Z-scan experiment graphs which were obtained with four different pulse energies. As shown in Figure 2, the curves are symmetrical on the beam waist, when the energies were relatively low (45 nJ and 90 nJ). The normalized transmissions of sample increase with laser energies, which indicate SA occurs in the sample. As shown in Figure 3, when the laser energies (110 nJ and 150 nJ) were relatively high, the curves show two peaks and a valley. It is well known that an increase in pulse energy can cause local thermo-optical effectors in solvents or nonlinear effects in quartz. The light energy used in this experiment is low, and the pulse repetition frequency is only 1 Hz, which is not enough to cause obvious photothermal phenomenon. As mentioned earlier, under our experimental intensity, there is no obvious nonlinearity in the quartz cell filled with ethanol. Therefore, we believe that the configuration with two peaks and valleys shows the switch from SA to RSA. It is also observed a similar switching in other nanoparticles [1–13].

Ganeev et al. used a nanosecond laser at 397.5 nm to study the nonlinear absorption of silver nanoparticles, and they obtained the result of pure saturated absorption [14]. Fan et al. used a femtosecond laser at 800 nm to study the nonlinear absorption of silver nanoparticles, and they also obtained pure saturated absorption [19]. The results of these related studies are the same as the results of our experiments under low intensity. The SPR peak of the Ag nanoparticles was located at 403 nm, and the wavelength of excitation laser is 400 nm. Therefore, SA was related to the ground state plasmon bleaching [14,15]. The increasing excitation flux causes the ground state plasma to bleach when the silver nanoparticles move towards the beam focus. The difference is that, when the excitation intensity is increased, RSA appears in our experiment. For Ag nanoparticles, the interband transition absorption band is at about 320 nm, corresponding energy is about 4.1 eV, which is larger than that of 400 nm laser (about 3.1 eV) [20–23]. Therefore, the interband transitions induced by two-photon absorption (TPA) can occur, which causes RSA [10,12,24].

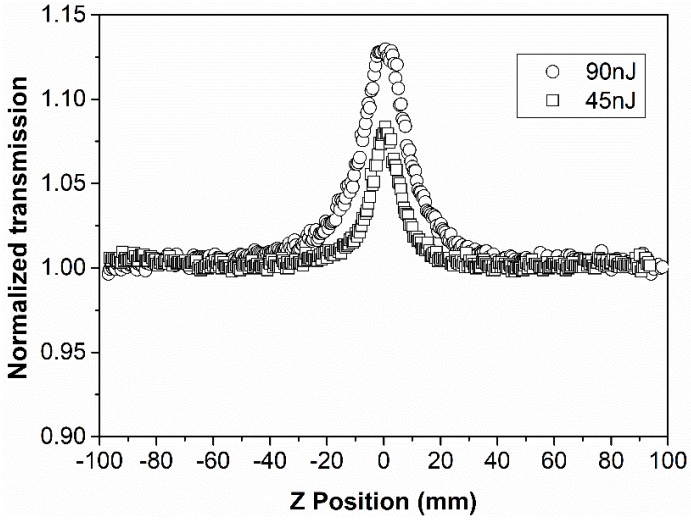

Figure 2. Single peak at relatively low energies (45 nJ and 90 nJ).

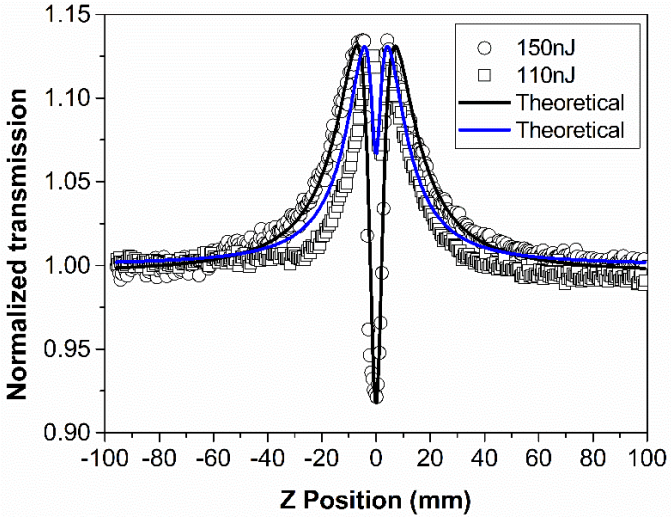

Figure 3. Double peak and a valley at relatively high laser energies (110 nJ and 150 nJ).

In open-aperture Z-scan experiments, normalized transmittance can be formulated as [17]

$$T(z) = \sum_{m=0}^{\infty} \frac{\left[-\beta I_0 L_{eff}/\left(1+z^2/z_0^2\right)\right]^m}{(m+1)^{\frac{3}{2}}} \quad (1)$$

where β is the TPA coefficient, I_0 represents on-axis laser intensity at the focus, $L_{eff} = [1-\exp(-\alpha_0 L)]/\alpha_0$ is length of effective interaction, L represents thickness of samples, α_0 represents the linear absorption coefficient, z represents distance of samples to focus ($z = 0$), z_0 represents Rayleigh diffraction size.

To analyze the switching of nonlinear absorption above, we define a non-linear absorption coefficient as below [24]

$$\alpha(I) = \frac{\alpha_0}{1+I/I_S} + \beta I \quad (2)$$

where α_0 represents linear absorption parameter, I_s intensity of saturation, I the laser intensity, and β is TPA coefficient. Thus, I can be expressed as

$$I = \frac{I_0}{1+z^2/z_0^2} \quad (3)$$

It can be simplified as

$$\alpha(I_0) = \frac{\alpha_0}{1 + \frac{I_0}{(1+z^2/z_0^2)I_s}} + \frac{\beta I_0}{1 + z^2/z_0^2} \quad (4)$$

In Equation (1), $\beta I_0/(1 + z^2/z_0^2)$ is replaced by Equation (4). Then the modified Equation (1) can be used to fit the experimental data. The coefficient of positive nonlinear absorption β and saturable intensity I_s were obtained to be 3.3×10^{-10} m/W and 1.3×10^{10} W/m^2, respectively. The theoretical curves are presented using solid line in Figure 3.

To evaluate the ultrafast response time and recovery time of the observed nonlinear absorption above, pump-probe experiment was carried out. The time ration $\Delta T/T$ is determined at various absorption energies of 30, 50, 80, and 100 nJ are displayed in Figure 4.

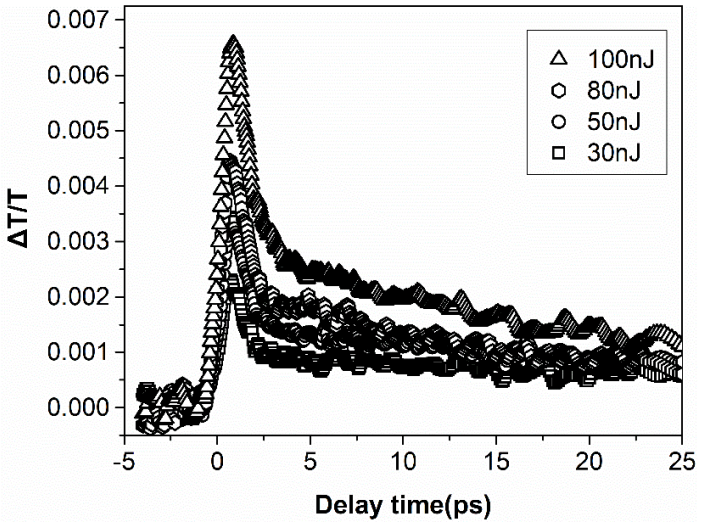

Figure 4. Transient differential transmissions $\Delta T/T$ determined at the pump energies of 100, 80, 50, and 30 nJ.

In Figure 4, it is observed that, following ultrafast laser excitation, there are a rapid ascent process and two decay ones, which is reported previously [25]. Specifically, the fast-rise signal origins from the ground status plasma of the system. We can find that the start-up time of the signal is larger than the FWHM of instrument response function (180 fs). Then $\Delta T/T$ value falls back in two different time scales, namely a fast one and a slow one. The process is 'two-exponential decay'. The fast decay is due to the electron–phonon (e–ph) coupling which causes energy leave the excited electron for the phonon. The following slow decay is a phonon–phonon (ph–ph) coupling process in which energy transfers to medium [26,27]. Then the equilibrium between the electrons and lattice is built. In Figure 4, it is found that, with the increase of pump energy from 30 nJ to 100 nJ, the transient bleach increases.

In Figure 5, the change of $\Delta T/T$ with pump energy is shown. Obviously, $\Delta T/T$ increase almost linearly with pump energy. As shown in Figure 6, The normalized transient differential transmission is given. It can be found that all signals are almost same, which implies pump fluence has no effect on decay rate. This is because the pump energies are low, which causes a low perturbation in measurements. In this regime, electron–phonon coupling can be determined precisely.

The transmittivity change ($\Delta T/T$) is an ultrafast energy relaxation process which can be evaluated using a bi-exponential decay function based on the two-temperature model

$$\frac{\Delta T}{T} = A_1 \exp(\frac{-t}{\tau_1}) + A_2 \exp(\frac{-t}{\tau_2}) \quad (5)$$

where τ_1, τ_2 and A_1, A_2 are the time constant and amplitude of two decays, respectively. The solid line in Figure 6 is theoretical fit of the experimental data by using Equation (5). As a result, the initial fast relaxation time $\tau_1 = (713 \pm 50)$ fs and a slow relaxation time $\tau_2 = (25.2 \pm 3)$ ps were obtained.

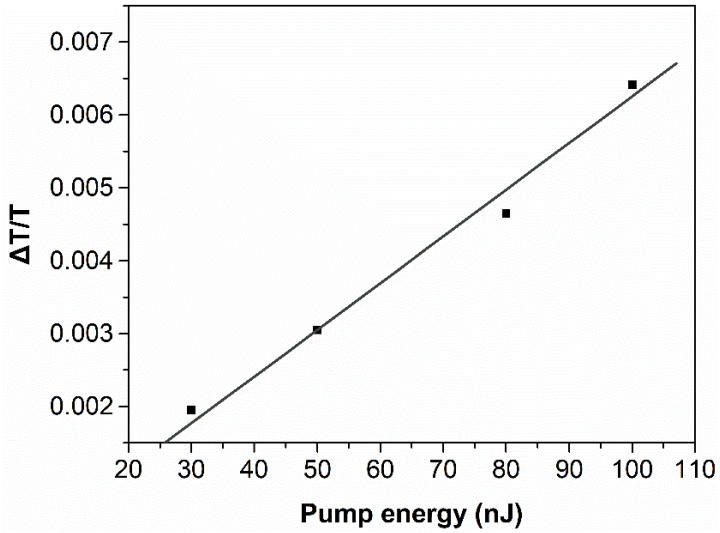

Figure 5. Pump pulse energy increases with peak value $\Delta T/T$.

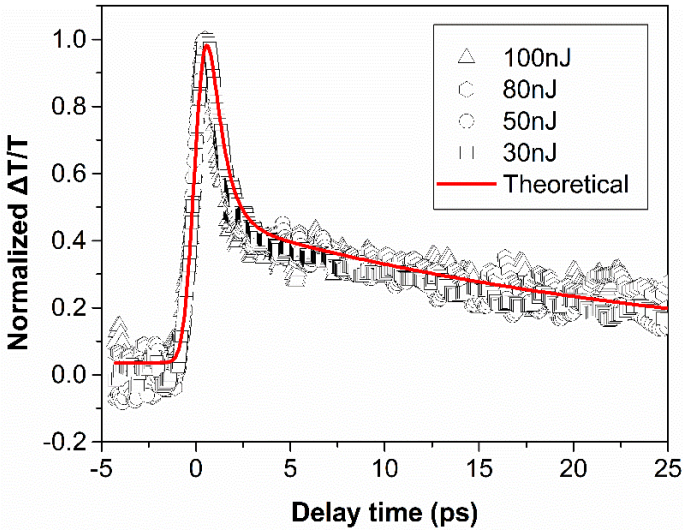

Figure 6. Normalized transient differential transmission at the different pump energies of 30, 50, 80, and 100 nJ.

A series of energy relaxation process occur under the excitation of light [26,27]. The first is the interaction between photons and electrons, and the electrons absorb the energy of the photons and become hot electron. Then, the energy exchange between electrons occurs. The third process is the lattice vibration caused by the temperature rise of hot electrons under the action of pulsed light, which is regarded as the interaction between electrons and phonons. The last process is the interaction of phonons and phonons, lattice

vibration transfers energy to the surrounding ethanol solvent. As the photon–electron and electron–electron relaxation is so quick that cannot be got using 130 fs laser. We believe $\tau_1 = (713 \pm 50)$ fs is e–ph relaxation time, $\tau_2 = (25.2 \pm 3)$ ps is ph–ph relaxation time. Relatively, the fast component contributes to the recovery of differential transmission signal more. The fast process time constant of 713 fs agrees with the value of 700 fs determined for 3 nm 'Ag clusters in a glass matrix' [26]. Arbouet et al. obtained a smaller time constant of approximately 530 fs for silver cluster of the same size in different medium [28]. It should be noted that although the 25 nm in our experiment and the 3 nm 'Ag clusters in a glass matrix' are different in size, the approximate e–ph relaxation time is obtained. Maurya et al. studied the size dependence of ultrafast dynamics of silver nanoparticles and found that the e–ph relaxation time ranges from 1.5 ps to 2.3 ps for nanoparticles with sizes ranging from 25 nm to 37 nm [29]. The size of the nanoparticles studied by Maurya et al. is not different from ours completely, but the e–ph relaxation time is different. We consider that the differences may be caused by the different preparation processes of Ag nanoparticles. After all, the crystal structure of the nanoparticles prepared by the laser ablation method and the chemical reduction method is different.

In addition, compared with bulk materials, the electron-phonon relaxation process in Ag nanoparticles is slow. This can be explained from two aspects: the quantization of the energy level of the silver nanoparticles and the vibrational dynamics density of the solvent around the silver nanoparticles. First, compared with bulk materials with band structures, the quantized energy level structure of nanoparticles may reduce the overall e–ph interaction, thereby slowing down the relaxation process. Secondly, silver nanoparticles are dispersed in ethanol solvent. Because the liquid vibration density is low and the contact between silver nanoparticles and the surrounding solvent is weak, this may cause the interaction between electrons and solvent to be weaker than that between electrons and bulk materials, thereby slowing down the relaxation process [30].

4. Conclusions

We investigated non-linear absorption and ultrafast relaxation dynamics of silver nanoparticles in ethanol solvent by 130 fs laser pulse at 400 nm. Our data showed that silver nanoparticles exhibit either SA or RSA under different laser intensities. The SA might be related to ground state plasma bleaching, while RSA results from TPA absorption. Saturable optical intensity I_s and TPA coefficient β determined to be 1.3×10^{10} W/m^2 and 3.2×10^{-10} m/W, respectively. Two component energy relaxations with the fast time constant $\tau_1 = (713 \pm 50)$ fs and the slower one $\tau_2 = (25.2 \pm 3)$ ps were demonstrated using pump-probe technique. The present results show Ag nanoparticle can be used as passive mode lockers and optical limiters in ultrafast lasers.

Author Contributions: Conceptualization, J.J. and Y.G.; Methodology, J.J. and Y.G.; Formal analysis, J.J. and J.W.; Investigation, J.J. and T.W.; Resources, Y.G.; Data curation, J.W. and T.W.; Writing—original draft preparation, J.J.; Writing—review and editing, Y.G.; Visualization, J.J.; Supervision, Y.G.; Project administration, Y.G. All authors have read and agreed to the published version of the manuscript.

Funding: This research was funded by the Natural Science Foundation of Heilongjiang Province, grant no. F2018027, LH2020F041, and LH2020E106, and the Fundamental Research Funds in Heilongjiang Provincial University (no. 135209239).

Data Availability Statement: Not applicable.

Conflicts of Interest: The authors declare no conflict of interest.

References

1. Elim, H.I.; Yang, J.; Lee, J.Y.; Mi, J.; Ji, W. Observation of saturable and reverse-saturable absorption at longitudinal surface plasmon resonance in gold nanorods. *Appl. Phys. Lett.* **2006**, *88*, 083107. [CrossRef]
2. Karthikeyan, B.; Anija, M.; Philip, R. In situ synthesis and nonlinear optical properties of Au:Ag nanocomposite polymer films. *Appl. Phys. Lett.* **2006**, *88*, 053104. [CrossRef]

3. Wu, D.J.; Liu, X.J.; Liu, L.L.; Qian, W.P. Third-order nonlinear optical properties of gold nanoshells in aqueous solution. *Appl. Phys. A* **2008**, *92*, 279–282. [CrossRef]
4. Polavarapu, L.; Xu, Q.H. A single-step synthesis of gold nanochains using an amino acid as a capping agent and characterization of their optical properties. *Nanotechnology* **2008**, *19*, 075601. [CrossRef]
5. Seo, J.T.; Yang, Q.; Kim, W.J.; Heo, J.; Temple, D. Optical nonlinearities of Au nanoparticles and Au/Ag coreshells. *Opt. Lett.* **2009**, *34*, 307–309. [CrossRef]
6. Lee, Y.H.; Yan, Y.; Polavarapu, L.; Xu, Q.H. Nonlinear optical switching behavior of Au nanocubes and nano-octahedra investigated by femtosecond Z-scan measurements. *Appl. Phys. Lett.* **2009**, *95*, 5233. [CrossRef]
7. Philip, R.; Ravindrakumar, G.; Sandhyarani, N.; Pradeep, T. Picosecond Optical Nonlinearity in Monolayer-Protected Gold, Silver, and Gold-Silver Alloy Nanoclusters. *Phys. Rev. B* **2000**, *62*, 13160. [CrossRef]
8. Gurudas, U.; Brooks, E.; Bubb, D.M.; Heiroth, S.; Lippert, T.; Wokaun, A. Saturable and reverse saturable absorption in silver nanodots at 532 nm using picosecond laser pulses. *J. Appl. Phys.* **2008**, *104*, 1541. [CrossRef]
9. Chan, Z.; Du, Y.; Feng, M.; Zhan, H. Shape dependence of nonlinear optical behaviors of nanostructured silver and their silica gel glass composites. *Appl. Phys. Lett.* **2008**, *93*, 17512.
10. Zheng, C.; Ye, X.Y.; Cai, S.G.; Wang, M.J.; Xiao, X.Q. Observation of nonlinear saturable and reverse-saturable absorption in silver nanowires and their silica gel glass composite. *Appl. Phys. B* **2010**, *101*, 835–840. [CrossRef]
11. Unnikrishnan, K.P.; Nampoori, V.; Ramakrishnan, V.; Umadevi, M.; Vallabhan, C. Nonlinear optical absorption in silver nanosol. *J. Phys. D* **2003**, *36*, 1242. [CrossRef]
12. Anija, M.; Thomas, J.; Singh, N.; Nair, A.S.; Tom, R.T.; Pradeep, T.; Philip, R. Nonlinear light transmission through oxide-protected Au and Ag nanoparticles: An investigation in the nanosecond domain. *Chem. Phys. Lett.* **2003**, *380*, 223–229. [CrossRef]
13. Yan, D.; Sun, Y.; Pei, W.; Zhang, D.; Jiao, X.; Hai, M.; Zhang, Q.; Yang, J.; Sun, X. Nonlinear optical properties of silver colloidal solution by in situ synthesis technique. *Curr. Appl. Phys.* **2008**, *8*, 13–17.
14. Ganeev, R.A.; Ryasnyansky, A.I. Nonlinear optical characteristics of nanoparticles in suspensions and solid matrices. *Appl. Phys. B* **2006**, *84*, 295–302. [CrossRef]
15. Gao, Y.; Wu, W.; Kong, D.; Ran, L.; Chang, Q.; Ye, H. Femtosecond nonlinear absorption of Ag nanoparticles at surface plasmon resonance. *Phys. Low Dimens. Syst. Nanostruct.* **2012**, *45*, 162–165. [CrossRef]
16. Iryo, K.; Watanabe, N.; Tsuji, M. Preparation of silver nanoparticles by laser ablation in solution: Influence of laser wavelength on particle size. *Appl. Surf. Sci.* **2002**, *202*, 80–85.
17. Sheik-Bahae, M.; Said, A.; Wei, T.H.; Hagan, D.J.; Stryland, E.V. Sensitive measurement of optical nonlinearities using a single beam. *IEEE J. Quantum Electron.* **2002**, *26*, 760–769. [CrossRef]
18. Chen, C.; Wang, J.; Yang, S.; Wu, W.; Kong, D. Ultrafast dynamics process of platinum nanoparticles under femtosecond laser. *J Nanopart. Res.* **2018**, *20*, 242. [CrossRef]
19. Fan, G.H.; Qu, S.L.; Guo, Z.Y.; Wang, Q.; Li, Z.G. Size-dependent nonlinear absorption and refraction of Ag nanoparticles excited by femtosecond lasers. *Chin. Phys. B* **2012**, *21*, 047804. [CrossRef]
20. Kreibig, U. Electronic properties of small silver particles: The optical constants and their temperature dependence. *J. Phys. F Met. Phys.* **2001**, *4*, 999–1014. [CrossRef]
21. Yang, L.; Osborne, D.H.; Haglund, R.F.; Magruder, R.H.; White, C.W.; Zuhr, R.A.; Hosono, H. Probing interface properties of nanocomposites by third-order nonlinear optics. *Appl. Phys. A* **1996**, *62*, 403–415. [CrossRef]
22. Uppenbrink, J.; Wales, D.J. Structure and dynamics of model metal clusters. *J. Chem. Phys.* **1993**, *98*, 5720–5733. [CrossRef]
23. Lehmann, J.; Merschdorf, M.; Pfeiffer, W.; Thon, A.; Voll, S.; Gerber, G. Surface Plasmon Dynamics in Silver Nanoparticles Studied by Femtosecond Time-Resolved Photoemission. *Phys. Rev. Lett.* **2000**, *85*, 2921–2924. [CrossRef] [PubMed]
24. Gao, Y.; Zhang, X.; Li, Y.; Liu, H.; Wang, Y.; Chang, Q.; Jiao, W.; Song, Y. Saturable absorption and reverse saturable absorption in platinum nanoparticles. *Opt. Commun.* **2005**, *251*, 429–433. [CrossRef]
25. Tanaka, I.K.; Tanahashi, I.; Hirao, K. Ultrafast dynamics of nonequilibrium electron in gold nanoparticle system. *Phys. Rev. B* **1998**, *57*, 11334–11340.
26. Fatti, N.D.; Vallée, F.; Flytzanis, C.; Hamanaka, Y.; Nakamura, A. Electron dynamics and surface plasmon resonance nonlinearities in metal nanoparticles. *Chem. Phys.* **2000**, *251*, 215–226. [CrossRef]
27. Jain, P.K.; Qian, W.; El-Sayed, M.A. Ultrafast electron relaxation dynamics in coupled metal nanoparticles in aggregates. *J. Phys. Chem. B* **2006**, *110*, 136–142. [CrossRef]
28. Arbouet, A.; Voisin, C.; Christofilos, D.; Langot, P.; Treguer, M. Electron-Phonon Scattering in Metal Clusters. *Phys. Rev. Lett.* **2003**, *90*, 177401. [CrossRef]
29. Maurya, S.K.; Rout, A.; Ganeev, R.A.; Guo, C. Effect of Size on the Saturable Absorption and Reverse Saturable Absorption in Silver Nanoparticle and Ultrafast Dynamics at 400 nm. *J. Nanomater.* **2019**, *10*, 103201. [CrossRef]
30. Roberti, T.W.; Smith, B.A.; Zhang, J.Z. Ultrafast electron dynamics at the liquid–metal interface: Femtosecond studies using surface plasmons in aqueous silver colloid. *J. Chem. Phys.* **1995**, *102*, 3860–3866. [CrossRef]